Optik 130 (2017) 757–764

Contents lists available at ScienceDirect

Optik

journal homepage: www.elsevier.de/ijleo

Original research article

Pulsar profile denoising using kernel regression based on maximum correntropy criterion

Yidi Wang*, Wei Zheng, Dapeng Zhang, Lu Zhang

College of Aerospace Science and Engineering, National University of Defense Technology, Changsha 410073, China

ARTICLE INFO

Article history:
Received 6 September 2016
Accepted 31 October 2016

Keywords:
X-ray pulsar-based navigation
Kernel regression
Correntropy

ABSTRACT

A pulsar profile denoising method using kernel regression based on maximum correntropy criterion is proposed. This method uses the kernel regression to reduce the human visual inspection inescapable in the current profile denoising methods and the reliance of the prior knowledge on the profile of interest. In order to cope with the non-Gaussian case that is common in a real application, the maximum correntropy criterion is introduced into the kernel regression to resist the impact of non-Gaussian noise. The performance of the prosed method is verified via simulation and real data. The results have shown that the proposed method outperforms the current signal denoising methods in a non-Gaussian environment and is readily to be applied.

1. Introduction

Pulsar is a type of rapidly spinning neutron star that emits electromagnetic radiation through its magnetic poles [1]. A measurement device can receive a pulsed signal, when the electromagnetic radiation sweeps across the device. Since the discovery of the pulsar, scientists and scholars have gradually realized that the pulsar can be employed as a 'perfect' natural clock as it has a brilliant long-term periodicity stability that can match the current atomic clock. The concept of pulsar-based autonomous navigation was first introduced in 1970s [2]. The concept has experienced a sharp growth, bringing in a nearly-complete framework. Since 1993, the United States has performed a series of programs on pulsar-based navigation method, especially the ongoing SEXTANT program planned to verify the pulsar-based navigation system on the International Space Station (ISS) in 2016 [3]. The European Space Agency (ESA) analyzed the feasibility of pulsar-based navigation method in 2004 [4]. The study on pulsar-based navigation has attracted numbers of researchers in China and arose some heuristic works [5,6].

According to the energy band of electromagnetic radiation, the pulsar can be categorized as X-ray pulsar, radio pulsar, γ-ray pulsar and et al. In order to reduce the size and power consumption of satellite-borne sensor, the X-ray pulsar is recommended to be utilized for navigation. Although the signal of X-ray pulsar is claimed to be a pulse, a spacecraft can merely record a series of discrete photon time of arrivals (TOAs), as the flux of an X-ray pulsar is extremely weak [7]. In order to analyze the character of the pulsar signal and to calculate the pulse TOA, an empirical profile of pulsar must be recovered using the recorded photon TOAs. The predominant method for profile recovery is called epoch folding, which would be renamed direct epoch folding (DEF) in the remainder of the paper [8]. DEF is consisted of the following three steps: 1) fold the photon TOAs recorded over the whole observation period of pulsar back into the first period; 2) divide the first

* Corresponding author.
E-mail address: wangyidi19860609@163.com (Y. Wang).

http://dx.doi.org/10.1016/j.ijleo.2016.10.132
0030-4026/

period into N_b bins with equal length and count the photons falling into each bin; and 3) normalize the empirical profile using the number of all recorded photons [9] pointed out that the difference between the empirical and the true profile (i.e. DEF noise), can be modeled as a zero-mean Gaussian noise, the standard deviation of which is a term of N_b. In order to investigate the detailed information within the empirical profile and to have a high-precision pulse TOA, N_b is expected to be as large as possible. However, the growth of N_b increases the DEF noise. Although the DEF noise would be reduced by prolonging the observation period of pulsar in theory, a spacecraft is hardly to observe a specific pulsar for a long time as the spacecraft keeps performing an orbital motion. In this case, it is necessary to develop methods to enhance the signal to noise ratio (SNR) of the recovered empirical profile.

There are two main types of ways to realize the above objective: 1) fitting the empirical profile using a Gaussian mixture model [10]; and 2) signal denoising such as wavelet-based method and empirical model decomposition (EMD) [11]. In essence, the two ways belong to parametric regression that presets the empirical profile as a sum of a series of base functions weighted by coefficients needed to be fitted. The performance of the methods heavily relies on whether the presumed models are accurate enough to describe the empirical profile. In addition, the signal denoising methods needs to empirically set the signal decomposition level that determines whether the high-frequency noise can be removed. Thus, the aforementioned methods are more suitable for off-line analysis rather than for on-orbit autonomous operation of spacecraft, as they are interactive or need human visual inspection.

On the other hand, the assumption that DEF noise is Gaussian holds only when the X-ray detector works well over the whole observation period. If some problems, such as the atomic clock cannot provide accurate time sampling caused by the clock drift or color noise, occur in the X-ray detector, it would cause a pseudo-photon case, where the detector would record not only the photons from the pulsar as well as the pseudo-photons produced by the detector itself. In other words, the detector would record photons more than the ordinary case. In this case, the DEF noise becomes a non-Gaussian noise. Although, based on the central limit theorem, the noise could be approximated as a Gaussian one when the observation period is long enough, a spacecraft cannot observe a specific pulsar for a long time as described before. In a non-Gaussian environment, the performance of aforementioned methods would fall, as the weights in the methods are calculated out using least square that is vulnerable to the presence of non-Gaussian noise.

Thus, for X-ray pulsar-based navigation, it is necessary to propose a signal denoising method that can autonomously perform and resist to the impact of non-Gaussian noise. In this paper, we propose a kernel regression based on maximum correntropy criterion to accomplish the above objective. Kernel regression is a typical non-parameteric regression method that expresses the measurement at an arbitrary epoch as a sum of the measurements at the past epochs weighted by kernel functions [12]. However, the kernel regression is also easily affected by non-Gaussian noise, as the kernel regression works based on the minimum mean square error criterion (MMSEC). To cope with the non-Gaussian noise, we modify the MMSEC to be the maximum correntropy criterion (MCC), as the correntropy is a generalized correlation function that has been documented to perform better than correlation function in a non-Gaussian noise environment [13]. Compared with Gaussian mixture model and current signal denoising method, the proposed method requires little prior knowledge of the investigated signal and does not need to set decomposition level in advance.

The remainder of this paper proceeds as follows. Section 2 introduces the related works. Section 3 shows how to embed the MCC into the kernel regression. Section 4 analyzes the performance of proposed method via simulation, and Section 5 investigates the performance via the experiment data from Rossi X-ray Timing Explorer (RXTE).

2. Related works

2.1. Kernel regression

Assuming a nonlinear model is

$$\boldsymbol{y} = \boldsymbol{s}(\boldsymbol{X}) + \boldsymbol{\omega}, \tag{1}$$

where $\mathbf{y} \in \mathbb{R}^{n\times 1}$ is the measurement, $\mathbf{X} \in \mathbb{R}^{n\times 1}$ is the vector of measurement epoch, and $\boldsymbol{\omega}$ is the measurement noise.

Then, using the kernel regression, the estimate of $\mathbf{y}$ at x, $\hat{\boldsymbol{y}}$, can be obtained by solving the minimizing problem of [12]

$$\hat{\boldsymbol{y}} = arg\min \sum_{i=1}^{n} \left(y_i - \hat{y}_i\right)^2 w_i(x), \tag{2}$$

where $\hat{y}_i$ is the ith component of $\hat{\boldsymbol{y}}$ and $w_i(x)$ is the weight with the expression of

$$w_i(x) = \kappa\left(\frac{x - X_i}{h}\right) / \sum_{i=1}^{n} \kappa\left(\frac{x - X_i}{h}\right). \tag{3}$$

In Eq. (3), $\kappa(\bullet)$ is the kernel function with a kernel width of h that can be autonomously calculated via Leave One Out Cross Validation.

As the expression of kernel function puts little impact on the final estimate result, Gaussian kernel function as shown in Eq. (4) is commonly used.

$$\kappa_G(t) = \frac{1}{\sqrt{2\pi}h}\exp\left(-\frac{t^2}{2h^2}\right) \tag{4}$$

As shown in Eq. (2), kernel regression provides the estimate at the epoch of interest without presetting a parametric model and the detailed expression of the estimate depends on the past measurements. Thus, the kernel regression could reduce the requirement on the prior knowledge of signal of interest and reduce the human interruption.

It can also be seen from Eq. (2), the solution of kernel regression is based on the MMSEC and is obtained by solving a locally-weighted least square problem in which $w_i(x)$ controls the region of neighboring area. However, MMSEC is widely documented to be vulnerable to the presence of non-Gaussian noise. Therefore, some criterion robust to the non-Gaussian noise is needed to enhance the performance of kernel regression facing a non-Gaussian environment.

2.2. Maximum correntropy criterion

When there are random variables $\boldsymbol{X}$ and $\boldsymbol{Y}$, the correntropy is defined as [13]

$$V(\boldsymbol{X},\boldsymbol{Y}) = E_{\boldsymbol{X},\boldsymbol{Y}}[\kappa(\boldsymbol{X},\boldsymbol{Y})] = \iint \kappa(x,y)\,dF_{\boldsymbol{X},\boldsymbol{Y}}(x,y), \tag{5}$$

where $E[\bullet]$ is the expectation operation, $\kappa(\bullet)$ is the kernel function, and $F_{\mathbf{X},\mathbf{Y}}(x,y)$ is the joint probability density function of $\boldsymbol{X}$ and $\boldsymbol{Y}$.

In practice, the joint probability density function is usually unknown and only finite number of data samples $\{(x_i,y_i), i=1,2,\cdots,N\}$ is available. In this case, correntropy can be computed by

$$\tilde{V}(\boldsymbol{X},\boldsymbol{Y}) = \frac{1}{N}\sum_{i=1}^{N}\kappa(x_i,y_i). \tag{6}$$

Assuming $e_i = x_i - y_i$, the Gaussian kernel function shown in Eq. (4) can be also used to calculate the correntropy. It follows from Eq. (6), $\kappa_G(e_i)$ reaches to its maximum when $e_i = 0$. Thus, the cost function that incarnates the maximum correntropy criterion is [14]

$$J_{MCC} = \min\left(\sum_{i=1}^{N}(\kappa_G(0) - \kappa_G(e_i))\right). \tag{7}$$

3. Modified kernel regression using MCC

Substituting Eq. (7) into Eq. (2), we could have the cost function of kernel regression based on MCC, i.e.,

$$J_{K,MCC} = \sum_{i=1}^{n}\left(\kappa_G(0) - \kappa_G\left(y_i - \hat{y}_i\right)\right)w_i(x). \tag{8}$$

Differentiating Eq. (8) with respect to $\hat{y}_i$ yields

$$\sum_{i=1}^{n}\frac{\kappa_G'\left(y_i-\hat{y}_i\right)}{y_i-\hat{y}_i}w_i(x)\left(y_i-\hat{y}_i\right) = 0. \tag{9}$$

Presuming the estimate error $r_i = \hat{y}_i - y_i$, we further enhance the robustness of kernel regression using the median of the estimate error to normalize it. We have

$$\bar{r}_i = \frac{r_i}{median(\mathbf{r})}, \tag{10}$$

where $\mathbf{r}$ is the estimate error vector and $median(\mathbf{r})$ is the median of $\mathbf{r}$.

Let

$$\psi_i = \frac{\kappa_G'(\bar{r}_i)}{\bar{r}_i}, \tag{11}$$

Eq. (10) can be modified as

$$\sum_{i=1}^{n}\psi_i w_i(x)\left(y_i-\hat{y}_i\right) = 0. \tag{12}$$

Table 1
Simulation conditions.

		PSR B0531+21	PSR B1821-24
Signal	Period [ms]	33.4	3.05
	Mean flux rate of pulsar [ph/s]	660 [14]	1.93 [15]
	Mean flux rate of background [ph/s]	13,860.2 [14]	50 [15]
Observation period [s]		500	3600
N_b		10,000	1000

Interestingly, Eq. (12) can be viewed as the derivative of the following cost function

$$\tilde{J}_{K,MCC} = \sum_{i=1}^{n} \psi_i w_i(x) \left(y_i - \hat{y}_i\right)^2. \tag{13}$$

Compared with Eqs. (2), (13) can be viewed as a further weighting minimum square error criterion. Thus, the kernel regression based on MCC can be solved using iterative least square algorithm. $\hat{\boldsymbol{y}}$ can be obtained by the following steps:

Step 1 obtain an initial estimate of $\mathbf{y}$, $\hat{\boldsymbol{y}}$, by solving Eq. (2).

Step 2 calculate ψ_i using Eqs. (10) and (11).

Step 3 recalculate $\hat{\boldsymbol{y}}$ by solving Eq. (13).

Although it seems that the operation of kernel regression based on MCC needs numerous iterations, once iteration is sufficient to guarantee a satisfactory result, according to the scholars' experience as well as the practice.

4. Application to the simulated data

In order to fully investigate the performance of the proposed method, we simulate the data of two X-ray pulsars (i.e., PSR B0531+21 and PSR B1821-24). The simulation conditions are shown in Table 1. There are five methods await to be compared, including the wavelet denoising with soft threshold (WDST), EMD, DEF, the kernel regression (KR), and the proposed method. For WDST, the wavelet 'db5' is used, and the decomposition level is 4.

The performance of methods would be analyzed two aspects including SNR and signal fidelity. We propose two merits to scale the signal fidelity:

1) Relative error of denoised profile, e_r. The relative error can be measured by

$$e_r = \sqrt{\sum_{i=1}^{N_b} \left(\tilde{\lambda}(\phi_i) - \lambda(\phi_i)\right)^2 / \sum_{i=1}^{N_b} \lambda^2(\phi_i)} \times 100\%, \tag{14}$$

where $\tilde{\lambda}(\phi_i)$ is the denoised profile at the ith Bin and the $\lambda(\phi_i)$ is the standard profile that can be viewed as the perfect result of denoising.

2) Initial phase offset between the denoised profile and the standard profile, $\Delta\phi$. $\Delta\phi$ can be calculated using cross-correlation method. In this paper, $\Delta\phi$ is obtained as a result of 1000 Monte Carlo simulations.

The standard profile of PSR B0531+21 and of PSR B1821-24 are obtained from [15] and [16] respectively. The photon TOAs are simulated according to the method shown in [17]. When observing the PSR B0531+21, the X-ray detector is assumed to fault over [30s,40s]. When observing the PSR B1821-24, the X-ray detector is assumed to fault over [50s,60s]. When the detector faults, the flux rate of pseudo-photon is assumed to be 100 ph/s.

Figs. 1 and 2 show the resulting profiles obtained from the six methods for two pulsars. Compared with the result of DEF, the proposed method, KR, WDST and EMD all can reduce the impact of DEF noise. In addition, the proposed method outperforms the other methods, as its result is much smoother.

Table 2 shows the SNRs, e_rs, and $\Delta\phi$s obtained from the five methods. In the Table 2, "pulsar 1" refers to PSR B0531+21 and "pulsar 2" refers to PSR B1821-24. Compared with DEF, the proposed method, KR, WDST, and EMD could all enhance SNR of empirical profile and reduce e_r. In addition, The performance of the proposed method is best among the five methods as it could achieve the highest SNR as well as the smallest e_r and $\Delta\phi$.

The comparison between the result of PSR B0531+21 and PSR B1821-24 illustrates that the performance of a signal denoising method is constrained by the flux of pulsar and of background. For a pulsar with comparatively large flux such as PSR B0531+21, SNR of empirical profile can be greatly enhanced via signal denoising methods. For a faint pulsar such as PSR B1821-24, the signal denoising methods do not work well.

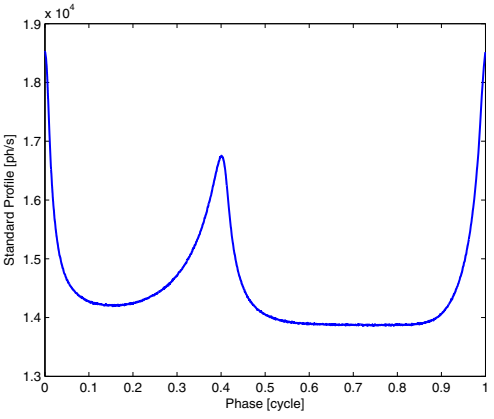

(a)

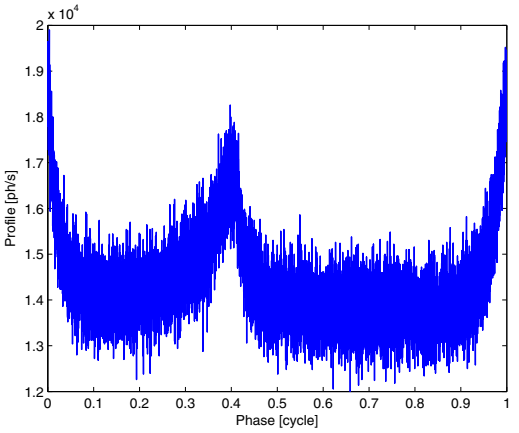

(b)

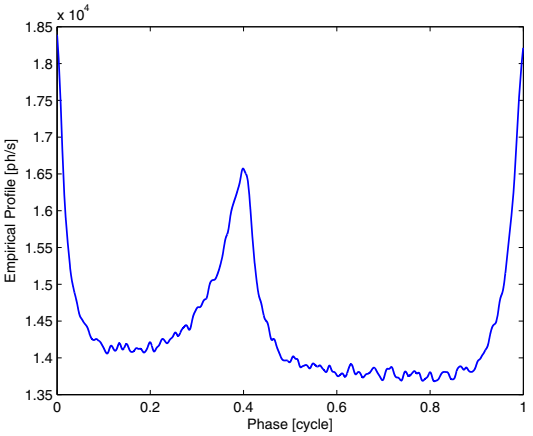

(c)

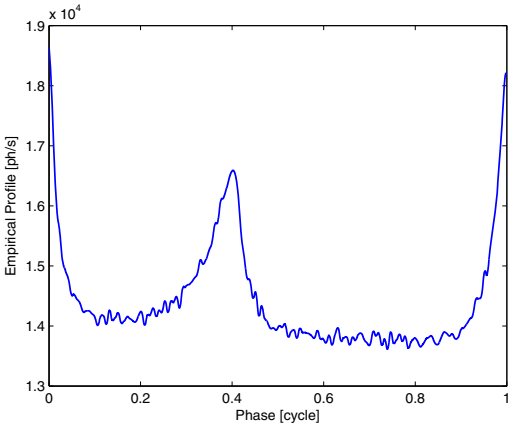

(d)

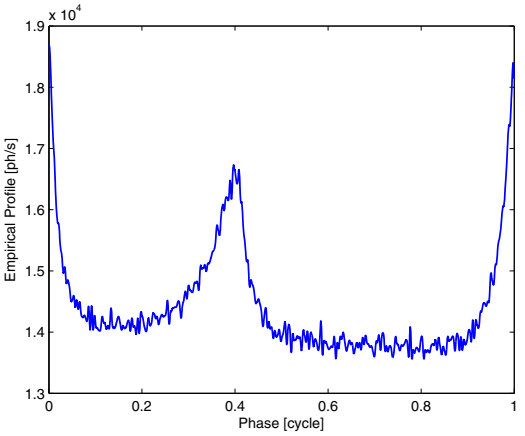

(e)

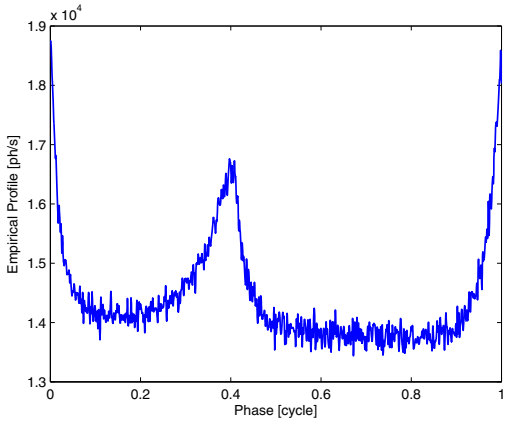

(f)

Fig. 1. Recovered profile of PSR B0531+21: (a) Standard profile; (b) result of DEF; (c) result of the proposed method; (d) result of KR; (e) result of WDST; and (f) result of EMD.

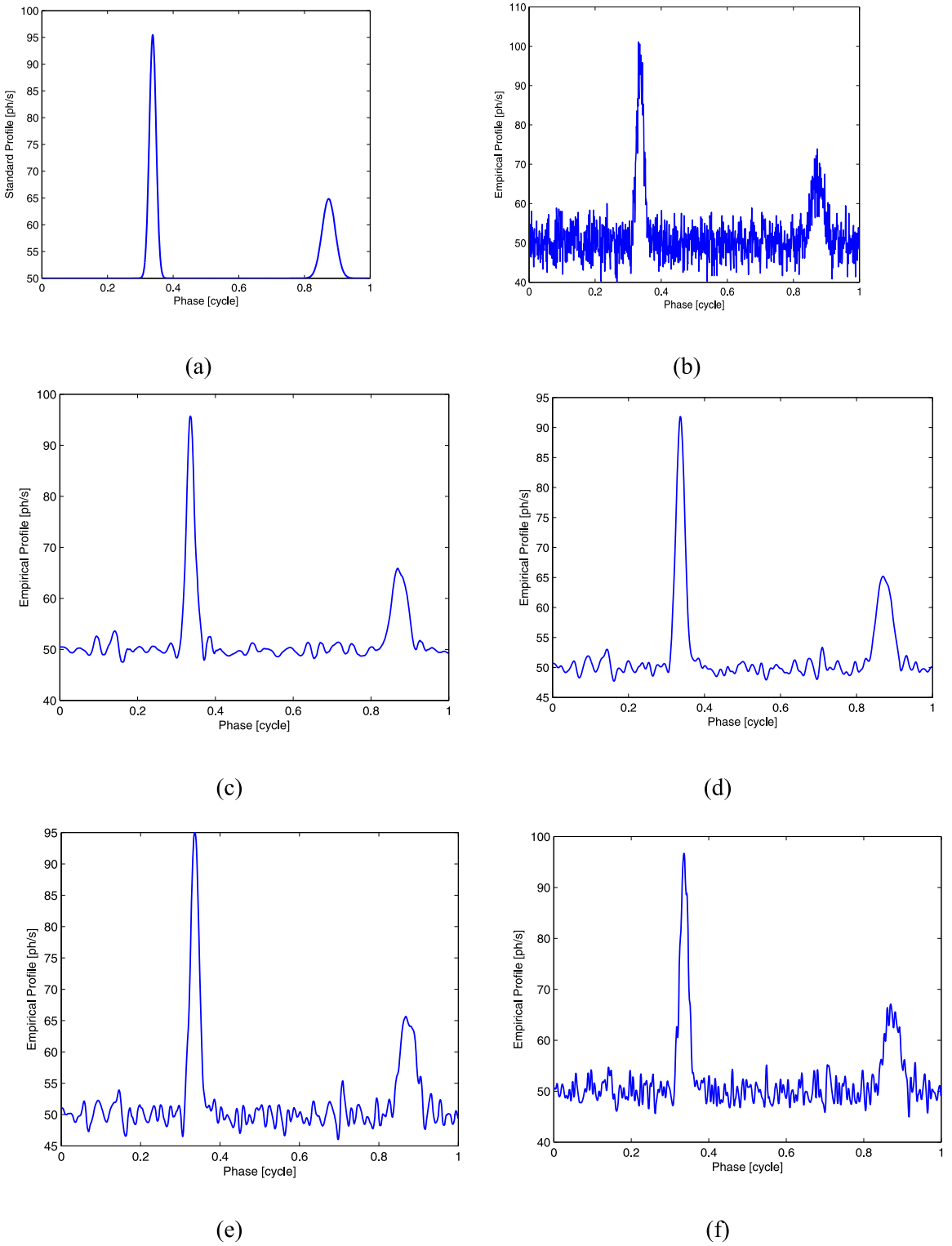

Fig. 2. Recovered profile of PSR B1821-24: (a) Standard profile; (b) result of DEF; (c) result of the proposed method; (d) result of KR; (e) result of WDST; and (f) result of EMD.

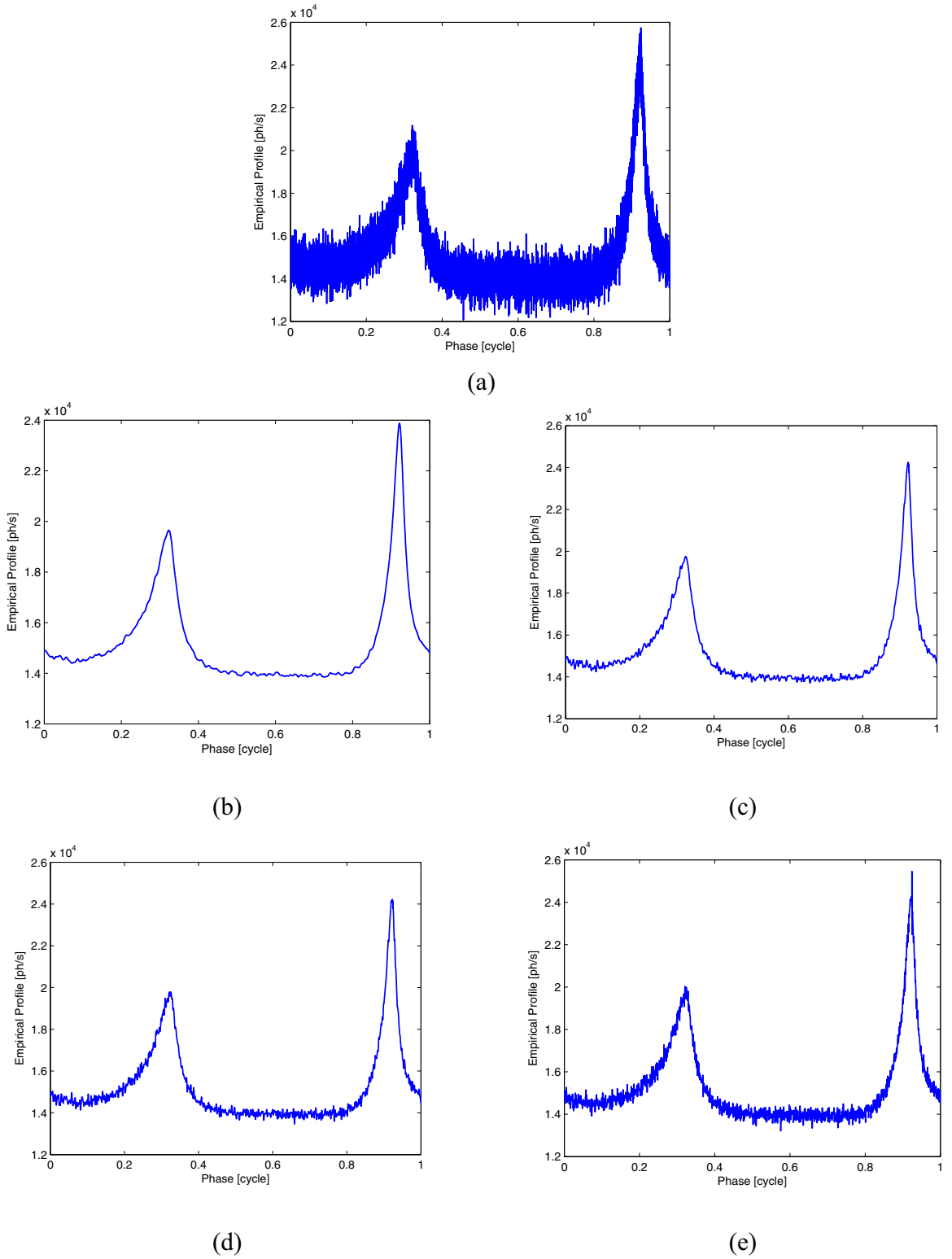

Fig. 3. Recovered profile via data of RXTE satellite: (a) Standard profile; (b) result of the proposed method; (c) result of KR; (d) result of WDST; and (e) result of EMD.

Table 2
Performance of the five methods.

	SNR [dB]		e_r [%]		$\Delta\phi$ [cycle]	
	Pulsar 1	Pulsar 2	Pulsar 1	Pulsar 2	Pulsar 1	Pulsar 2
Proposed method	21.56	17.97	0.77	1.9	3.4×10^{-5}	1.1×10^{-3}
KR	19.97	16.01	0.9	2.1	4.6×10^{-5}	1.3×10^{-3}
WDST	19.6	15.8	0.93	2.34	5.86×10^{-5}	1.46×10^{-3}
EMD	19.43	14.98	0.98	2.86	6.16×10^{-5}	1.53×10^{-3}
DEF	13.18	10.38	4.12	7.45	2.26×10^{-4}	2.3×10^{-3}

5. Application to the real data

The RXTE is the X-ray observation satellite launched by National Aeronautics and Space Administration (NASA) in 1995, and has a high temporal resolution of 1 μs [18]. RXTE has accomplished an X-ray survey and accumulated data of X-ray pulsars. This section employs the real data from the Proportional Count Array (PCA) in the RXTE to further testify the performance of the proposed method. Since the RXTE uses a medial-precision crystal oscillator without correcting by Global Positioning System (GPS) to maintain the on-board time system, the DEF recovered empirical profile is reasonable to be assumed as a non-Gaussian noise.

The data package of PSR B0531+21, 20804-01-04-00, is used. Firstly, the software Heasoft is employed to filter appropriate time interval, obtaining the photon TOAs at the Solar System Barycenter (SSB) using barycenter correction. Secondly, the period of the pulsar is found using χ^2 search method. Thirdly, an empirical profile is recovered using the searched period and DEF. The observation data lasting for 1000s is employed. And N_b is set as 10,000 in the process of DEF.

Fig. 3 provides the results of DEF, proposed method, KR, WDST and EMD. In practice, the DEF noise is too be ideal to be assumed as Gaussian noise. Compared with the result of DEF, the proposed method, KR, WDST and EMD can all achieve a profile with higher SNR. In addition, the result of proposed method could provide a profile smoother than the others.

6. Conclusions

This paper provides a pulsar profile denoising method using kernel regression based on maximum correntropy criterion. This method uses the kernel regression to overcome the problems in the current profile denoising methods, such as requiring high-precision prior knowledge of the investigated empirical profile and human visual inspection. Given that the noise within an empirical profile would be non-Gaussian in the real applications, the maximum correntropy criterion is introduced into the kernel regression to resist the impact of non-Gaussian noise. The performance of the prosed method is verified via simulation and real data. The results have shown that the proposed method outperforms the current wavelet-based method as well as the empirical model decomposition in a non-Gaussian environment.

References

[1] D. Lorimer, M. Kramer, Handbook of Pulsar Astronomy, Cambridge University Press, 2005.
[2] G. Downs, Interplanetary Navigation Using Pulsation Radio Sources. Report to NASA (1974).
[3] L.M.B. Winternitz, M.A. Hassouneh, J.W. Mitchell, and et al., X-ray Pulsar Navigation Algorithms and Testbed for SEXTANT, Technical Report to NASA (2015).
[4] J. Sala, A. Urruela, X. Villares, and et al., Feasibility Study for a Spacecraft Navigation System Relying on Pulsar Timing Information. ARIADNA Study 03/4202 (2004).
[5] W. Zheng, Y.D. Wang, J.G. Jiang, L. Liu, X-ray Pulsar-Based Navigation: Theory and Application, 1st edition, Science Press, 2015, 2016.
[6] Y.D. Wang, W. Zheng, S.M. Sun, et al., X-ray pulsar-based navigation using time-differenced measurement, Aerosp. Sci. Technol. 36 (2014) 27–35.
[7] H.F. Sun, W.M. Bao, H.Y. Fang, X.P. Li, Effect of stability of X-ray pulsar profiles on range measurement accuracy in X-ray pulsar navigation, Acta Phys. Sin. 63 (6) (2014) 069701.
[8] A. Emadzadeh, J. Speyer, X-ray pulsar-based relative navigation using epoch folding, IEEE Trans. Aerosp. Electron. Syst. 47 (4) (2011) 2317–2328.
[9] A. Emadzadeh, J. Speyer, On modeling and pulse phase estimation of X-ray pulsars, IEEE Trans. Signal Process. 58 (9) (2010) 4484–4495.
[10] H. Zhang, L.P. Xu, Y.H. Shen, et al., A new maximum-likelihood phase estimation method for X-ray pulsar signals, J. Zhejiang Univ. Sci. C 15 (6) (2014) 458–469.
[11] M.F. Xue, X. Li, Y. Liu, et al., Denoising of X-ray pulsar observed profile using biothogonal lifting wavelet transform, J. Syst. Eng. Electron. 27 (3) (2016) 514–523.
[12] H. Takeda, S. Farsiu, P. Milanfar, Kernel regression for image processing and reconstruction, IEEE Trans. Image Process. 16 (2) (2007) 349–366.
[13] J.C. Principe, Information Theoretic Learning-Renyi's Entropy and Kernel Perspectives, Springer, New York, 2010.
[14] I. Santamaria, P. Pokharel, J. Principe, Generalized correlation function: definition, properties and application to blind equalization, IEEE Trans. Signal Process. 54 (6) (2006) 2187–2197.
[15] M.Y. Ge, The X-ray Emission of Pulsars, Ph.D. Dissertation, Graduate university of Chinese academy of sciences, China, 2012.
[16] R. Rutledge, D. Fox, S. Kullkarni, et al., Micro-second timing of PSR B1821-24 with chandra/HRC-S, Astrophys. J. 613 (2004) 522–531.
[17] A. Emadzadeh, J. Speyer, Navigation in Space by X-ray Pulsars, Springer Press, 2010.
[18] S. Sheikh, D. Pines, P. Ray, Spacecraft navigation using X-ray pulsars, J. Guid. Control Dyn. 29 (2006) 49–63.